Fueling from the Electrochemistry of Halide Solid Electrolytes

Branimir Stamenkovic, Ying Shirley Meng, Philippe Moreau, Joel Gaubicher

Journal of The
Electrochemical Society

Communication—Fueling from the Electrochemistry of Halide Solid Electrolytes

To cite this article: Branimir Stamenkovic *et al* 2024 *J. Electrochem. Soc.* **171** 050554

Journal of The Electrochemical Society, 2024 **171** 050554

Communication—Fueling from the Electrochemistry of Halide Solid Electrolytes

Branimir Stamenkovic,[1,2] Ying Shirley Meng,[3,4] Philippe Moreau,[1,2,z] and Joel Gaubicher[1,2,z]

[1]*Nantes Université, CNRS, Institut des Matériaux de Nantes Jean Rouxel, IMN, Nantes F-44000, France*
[2]*ALISTORE-ERI European Research Institute, FR CNRS 3104, F-80039 Amiens Cedex 1, France*
[3]*Department of NanoEngineering, University of California San Diego, La Jolla, California 92093, United States of America*
[4]*Pritzker School of Molecular Engineering, The University of Chicago, Chicago, Illinois 60637, United States of America*

Unveiling the electrochemistry of solid-state Li_2ZrCl_6 halide electrolyte, we reveal its triple function as an ion conductor and a supplementary reversible, and sacrificial, electron source/sink. This groundbreaking discovery leads to a remarkable long-term enhancement of the specific capacity of industry-relevant heavily loaded $LiFePO_4$ electrodes by several tens of percent, while significantly amplifying that of Si-based or anode-less full cells through effective compensation for side reactions. We show that these effects can potentially be tuned by adjusting the initial xLiCl-$ZrCl_4$ composition of the solid electrolyte, which may thus become a new and mighty parameter for balancing the two electrodes.
 [DOI: 10.1149/1945-7111/ad4c99]

Manuscript received April 26, 2024. Published May 28, 2024.

Supplementary material for this article is available online

All-Solid-State Batteries (ASSBs) stand poised to surpass the energy densities of Li-ion batteries and alleviate safety concerns.[1] Among diverse solid-state electrolytes (SSEs), halides, notably Li_2ZrCl_6 (LZC), exhibit stability window up to 4 V vs $Li^+/Li°$,[2,3] while Y-doped LZC showed a reversible electrochemical activity in this potential region.[4] Halide based active materials with $Ti^{IV/III/II}$ and $Fe^{III/II}$ redox centers have also been used in electrodes[5,6] and as SSE.[5] Yet, the untapped potential of the halides SSEs 4 V redox activity for enhancing overall performance of ASSB remains unexplored, diverging from their conventional use for ionic conduction. In this communication, we unveil remarkable enhancements in the specific capacity of $LiFePO_4$(LFP)-based cells driven by combined effects that concurrently address major issues in silicon and anode-less chemistry.

Experimental

Electrolyte synthesis and materials.—LiCl (>99%, Sigma Aldrich) was dried overnight at 160 °C under vacuum, and $ZrCl_4$ (98%, anhydrous, Sigma Aldrich) was used as received. Electrolytes of composition xLiCl-$ZrCl_4$ ((x = 0.4, 0.59, 0.8, 1, 2 and 3, referred to as L_xZC) were synthesized by ball milling stoichiometric amount of LiCl and $ZrCl_4$ over 50 h at 600 rpm, with a 15 min break between each 1 h cycle. Carbon coated $LiFePO_4$ was provided by Blue Solutions Company.

Electrode preparation.—$Li_{0.33}In$ composite anode was prepared by folding Li foil into an In foil in 2:98 weight ratio, which was hand mixed with Li_6PS_5Cl electrolyte (NEI Corporation) in 60:40 wt% ratio. Cathodes were prepared by 2 h of ball milling at 300 rpm of LZC, LFP and VGCF in following mass ratios: 59.7:33.3:7 or 44.7:50:5.3, to achieve 1–1.4 or 4.1 mAh cm^{-2} areal capacity of half cells, respectively, or 56.7:33.3:10 for cathode in anode-less configuration. Micro-Si composite anode was obtained by ball milling Li_6PS_5Cl and micro-Si powder (Alfa Aesar, 1–20 micron) in 50:50 weight ratio under the same conditions as for the cathode.

Half and full cells assembly.—40 mg of Li_6PS_5Cl was pressed at 125 MPa for 10 s between two Ti plungers (10 mm diameter) inside insulating PEEK cylinder, forming the first layer (LPSC layer) of separator, on top of which 40 mg of xLiCl-$ZrCl_4$ was pressed at 375 MPa for 1 min. Then, appropriate amount of specific composite cathode powder was placed on top the LZC layer, and either 30 mg of composite $Li_{0.33}In$/LPSC anode or appropriate amount of micro-Si/LPSC composite anode to achieve N/P ratio 3, was placed on top of the LPSC layer. Finally, the whole stack was pressed at 375 MPa for 3 min.

Electrochemical characterizations.—Each cell was placed in the in-house pressure device under an external pressure of 100 MPa. Galvanostatic tests were conducted between 2.5 and 3.8–4 V vs Li^+/Li to limit the LZC redox activity or 5 V vs Li^+/Li to trigger it. Currents are indicated in corresponding figures. Cyclic voltammetry was performed in a 2.5 V–5 V range at 0.1 mV s^{-1}. All tests were performed at room temperature using VMP3 (Bio-logic) potentiostat.

Electrochemical impedance spectroscopy.—Prior to EIS measurements 120 mg LxZC powder was cold pressed into pellet at 375 MPa for 3 min. A sinusoidal voltage of 10 mV amplitude was applied in the frequency range 100 mHz—1 MHz to the cell under 100 MPa stack pressure.

Results and Discussion

To demonstrate these benefits, we assembled cells integrating different composite cathodes (see Experimental section) in three different configurations as depicted in Fig. S1. These cells were charged either to 4 V (vs Li^+/Li; $Li_{0.33}In$ having a stable potential of 0.625 V vs Li^+/Li[7]), which is typical when cycling LFP active material,[8] or 5 V to purposely oxidize the halide electrolyte.[2] Under a 4 V charge, the typical LFP profile[8] delivers a high discharge capacity 150 mAh/g_{LFP}, (50 mAh/$g_{cathode}$) (Fig. 1a). However, after charging the cathode to 5 V, the LZC electroactivity occurs from approx. 3.7 V during the subsequent discharge, dramatically enhancing the cathode discharge capacity by 36%, to 68 mAh/$g_{cathode}$ (205 mAh/g_{LFP}). Moreover, the LFP discharge plateau at 3.4 V exhibited no signs of additional polarization. This demonstrates that while LZC can be advantageously used as a second 4 V active material, it appears to maintain its electrolyte properties. The combined electroactivity of LZC and LFP consistently surpassed that of LFP alone by 22% even after 110 cycles (Fig. 1b). Furthermore, upon 110 cycles, the 94% capacity retention of LFP confirms the enduring conduction property of this redox electrolyte and the compatibility of the

[z]E-mail: joel.gaubicher@cnrs-imn.fr; philippe.moreau@cnrs-imn.fr

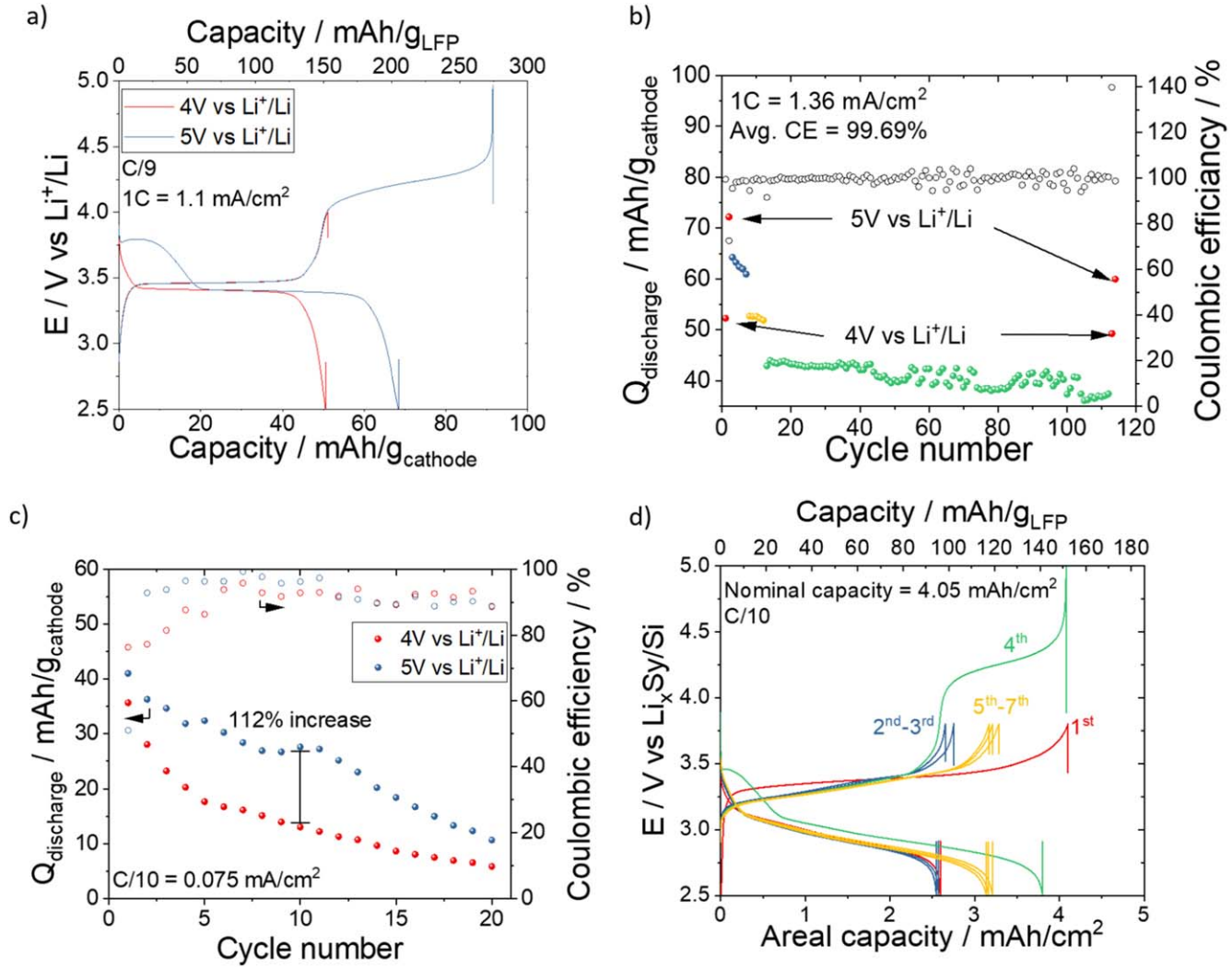

Figure 1. Electrochemical performance: (a)–(b) LZC-LFP /$Li_{0.33}In$ half cells at C/10 (red), C/5 (blue), C/2 (yellow) and C (green), coulombic efficiency (black), (c) anode-less/LZC-LFP and (d) micro-Si/LZC-LFP full cells.

LFP and LZC electrochemistry. Notably, LZC electroactivity led to the same capacity enhancement in the highly loaded cathode (4.1 mAh cm^{-2}) as shown in Fig. S2. In fact, triggering the LZC redox activity within such thick LFP electrode allows to reach nearly the same capacity (140 mAh/g_{LFP}) as that of LFP alone at five times higher C-rate (Fig. S2), and a capacity approx. 40% higher than a 1 mAh cm^{-2} electrode of similar composition but cycled up to 4 V.[8] Interestingly, the initial oxidation process is characterized by an irreversible decrease in cell pressure (Fig. S3a) despite Li alloying occurring at the negative electrode along with a significant increase in cell impedance (Fig. S3b). We hypothesize these results are indicative of substantial structural and morphological changes. However, strikingly, electrochemical impedance spectroscopy measurements of the reduced sample (Fig. S3b) indicate that cell impedance reverts to a value close to the pristine state, even after 10 cycles (Fig. S3b). This unexpected property is a crucial factor enabling LFP electrode to operate without additional polarization, regardless of whether the 4 V electrochemical activity of LZC is triggered or not (Fig. 1a).

Expanding on these discoveries, we delved into assessing the advantages of applying this approach to an anode-less configuration. Indeed, the inefficiency of lithium plating and stripping leads to pronounced capacity fading owing to the absence of excess lithium inventory.[9] Remarkably, triggering LZC 4 V electroactivity resulted in an astounding 112% capacity increase after 10 cycles, and greatly improved Coulombic efficicency (CE%) (Fig. 1c). Additionally, the effect on the cell safety and longevity, as dendrite-related irregularities were deferred from the second discharge to the tenth one (Fig. S4). These preliminary findings suggest the potential of halide electrochemistry for in situ deposition of a layer of lithium metal. When combined with other approaches[10] to further enhance capacity retention, this method would offer a solution to common issues encountered in negative electrode-less cell configurations.[11] Similarly, a Si-based full cell assembled at 4.1 mAh cm^{-2}, shows a 37% capacity loss during the initial cycle, coupled with low CE% (Fig. 1d). Given the anode/cathode ratio of 3 in this full cell, this drop of capacity is ascribed to side reactions stemming from reaction of Li_xSi with the argyrodite.[12] However, upon triggering LZC 4 V electroactivity, a remarkable 50% enhancement in discharge specific capacity was achieved. These improvements arise from two primary factors: the additional discharge capacity associated with LZC 4 V activity, and a larger capacity coming from LFP (Fig. 1d). Notably, a significant capacity gain directly linked to LFP persisted across subsequent cycles, even in the absence of the LZC redox process (Fig. 1d). Importantly, such capacity-loss healing can be harvested on demand by simply triggering the electrolyte at 5 V, suggesting that LZC oxidation can replenish the loss of active Li/e-.

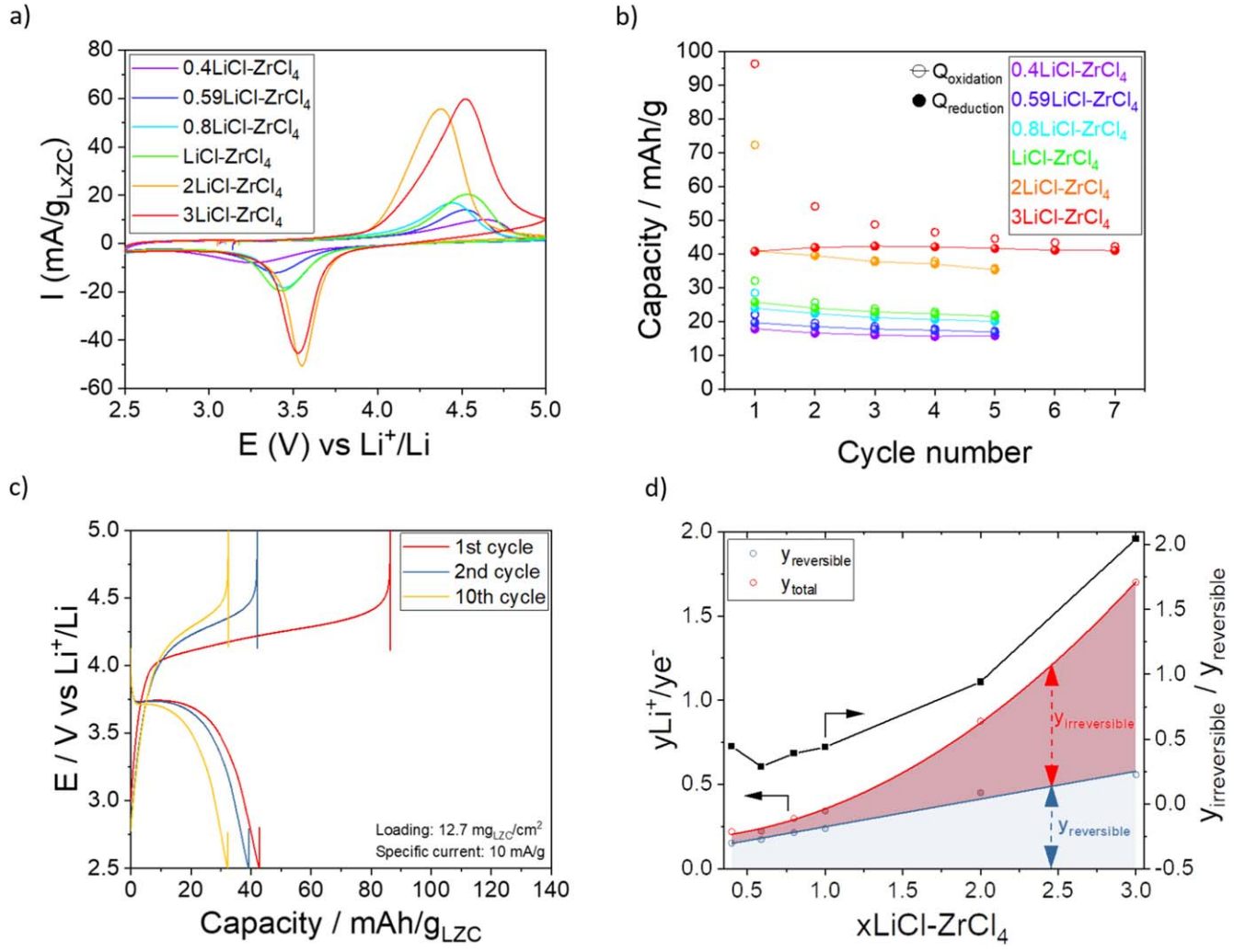

Figure 2. (a) Cyclic voltammograms of LixZC electrolytes at 0.1 mV s^{-1} and (b) corresponding capacity on cycling. (c) Galvanostatic profile of Li_2ZrCl_6 and (d) variations of reversible (blue) and total (reversible + irreversible) (red) capacities "y" as well as $y_{irreversible}/y_{reversible}$ against the compositions of the halide xLiCl-$ZrCl_4$. $y_{total} = y_{reversible} + y_{irreversible}$ with $y_{reversible}$ and $y_{irreversible}$ corresponding to the average reversible capacity and the sum of the irreversible capacity, respectively, over the number of cycles needed to reach a coulombic efficiency of 98% (Figs. S7a–S7b). y values have been calculated using the following equation: $y = \frac{(42.45x + 233.02)\frac{g_{Lx}ZC}{mol} \times \text{Capacity}\left(\frac{mAh}{g_{Lx}ZC}\right)}{0.0268\frac{mAh}{mol}}$.

In order to examine how the effects of this approach can be tailored, we investigated the reversible and irreversible aspects of LZC oxidation with respect to the cathode electrolyte composition. Regardless of the xLiCl-$ZrCl_4$ (LxZC) composition (XRD and conductivity characterizations as reported in Figs. S5 and S6 respectively), cyclic voltammetry evaluations revealed partially reversible faradic activity occurring at approximately 3.75 V (Fig. 2a). Interestingly both the discharge and charge capacities (Fig. 2b) follow an increasing trend with x. Moreover the 1st oxidation is systematically accompanied by the largest irreversibility (and lowest coulombic efficiency, CE%, Fig. S7a) that rapidly fades on cycling (Fig. 2b). In the case of Li_2ZrCl_6, the discharge capacity stabilizes above 30 mAh/g_{LZC} on cycling (Figs. 2c and S7b). This reversible capacity thus enables the enhancement of the positive LFP electrode's capacity that remains after 110 cycles (Fig. 1a), while the irreversible (sacrificial) capacity that is transferred to the negative electrode can be used to compensate for the loss of active Li/e- due to side reactions. Interestingly, the reversible and irreversible capacities show linear and parabolic relationships with the LxZC composition (Fig. 2d), respectively and the ratio of these two capacities significantly increases (by nearly 200%) from x = 0.4 to x = 3. Therefore by leveraging the chloride redox chemistry of LZC,[2] the non-stoichiometric composition of the halide electrolyte may thus become a new and potent parameter for electrode balancing. A comprehensive study aimed at gaining fundamental understanding of the controversial redox mechanisms,[2,13] as well as the related LZC structural and morphological changes remains crucial for further improvement of this approach.

Conclusions

By exploring the reversible and irreversible aspects of LZC oxidation occurring within the cathode above 4 V vs $Li^+/Li°$, we have uncovered its ability to serve as a supplementary reversible and sacrificial source of electrons and lithium ions while maintaining its role as electrolyte. These effects that can be tuned by adjusting the LZC initial composition, leads to a remarkable long-term enhancement of the specific capacity of $LiFePO_4$ (LFP)-based electrodes while effectively compensating for side reactions in silicon-based electrodes or anode-less full cells. We believe that the simplicity and versatility of this approach, demonstrated with highly loaded

electrodes, make it highly accessible for implementation in practical battery designs, further highlighting its potential for widespread adoption in the development of all-solid-state batteries (ASSBs).

Acknowledgments

As a part of the **DESTINY PhD program**, this publication is acknowledged by **funding from the European Union's Horizon2020** research and innovation program under the **Marie Skłodowska-Curie Actions COFUND (Grant Agreement #945357).** JG and PM acknowledge Dr Eric Quarez (IMN) for Rietveld refinement. Y.S.M thanks the University of Chicago - France program (FACCTS, 2023) for its financial support. IMN's group acknowledge Y.S.M's group and in particular S.-Yeon Ham and Ashley Cronk for training on manufacturing of ASSB.

ORCID

Ying Shirley Meng https://orcid.org/0000-0001-8936-8845
Philippe Moreau https://orcid.org/0000-0002-1691-1592
Joel Gaubicher https://orcid.org/0000-0001-6229-740X

References

1. J. Janek and W. G. Zeier, *Nat. Energy*, **1**, 1 (2016).
2. K. Wang et al., *Nat. Commun.*, **12**, 4410 (2021).
3. T. K. Schwietert, A. Vasileiadis, and M. Wagemaker, *JACS Au*, **1**, 1488 (2021).
4. S. Chen et al., *Energy Mater. Adv.*, **4**, 0019 (2023).
5. K. Wang, Z. Gu, Z. Xi, L. Hu, and C. Ma, *Nat. Commun.*, **14**, 1396 (2023).
6. N. Tanibata, M. Kato, S. Takimoto, H. Takeda, M. Nakayama, and H. Sumi, *Adv. Energy Sustain. Res.*, **1**, 2000025 (2020).
7. A. L. Santhosha, L. Medenbach, J. R. Buchheim, and P. Adelhelm, *Batter. Supercaps*, **2**, 524 (2019).
8. A. Cronk et al., *ACS Energy Lett.*, **8**, 827 (2023).
9. W.-Z. Huang et al., *Adv. Energy Mater.*, **12**, 2201044 (2022).
10. Y.-G. Lee et al., *Nat. Energy*, **5**, 299 (2020).
11. S.-Y. Ham, A. Cronk, Y. S. Meng, and J. Jang, *MRS Bull.*, **48**, 1269 (2023).
12. D. H.-S. Tan et al., *Science*, **373**, 1494 (2021).
13. Q. Shao et al., *ACS Appl. Mater. Interfaces*, **14**, 8095 (2022).